



Global Buckling Strength of Girts with Inner Flange in Compression

Huy Hoang Vu¹, Quoc Anh Vu^{1*}, Cao Hung Pham²

¹ Faculty of Civil Engineering, Hanoi Architectural University, Hanoi, Vietnam.

² School of Civil Engineering, The University of Sydney, Sydney NSW 2006, Australia.

Received 08 June 2024; Revised 12 October 2024; Accepted 19 October 2024; Published 01 November 2024

Abstract

The objective of this paper is to provide guidance on improving the lateral-torsional buckling strength of cold-formed, channel-section wall girts subjected to leeward wind loads, which cause the inner flange to compress. Additionally, it aims to identify the cross-sectional dimensions that most affect this strength. This is necessary due to the observation that the lateral-torsional buckling strength, with the inner flange in compression, of those members is significantly lower than that of the outer flange due to the difference in lateral bracing lengths, which leads to material waste. The available methods for improving the lateral-torsional buckling of girts when the inner flange is in compression were first summarized. Then, a parametric study was performed on three typical channel cross-sections. Sixty-three cases were created by varying flange width, lip length, cross-sectional depth, and thickness within practical ranges. These cases were solved manually for lateral-torsional buckling strengths using Microsoft Excel. The results showed that increasing the flange width is the most effective way to improve the flexural strength without considering the bracing effect of sheathings, M_{nl} , while increasing the cross-section thickness is the best for the strength considering the sheathing effect, M_n . Therefore, a new asymmetrical section with a larger inner flange width is recommended for girts when M_{nl} governs the strength.

Keywords: Girt; Cold-Formed; Lateral-Torsional; Global Buckling; Leeward Wind; Negative Pressure; Inner Flange.

1. Introduction

Wall girts in factory structures commonly use cold-formed C-section steel members due to their lightweight nature and easy fabrication. The primary loads acting on wall girts are wind loads in two opposite directions, windward and leeward, so the major axis of the section is oriented vertically to sustain these loads. These two directions of wind load cause either flange to be compressive. For example, in the most common simply-supported girts, the windward load causes the outer flange, which is fastened to the sheathing, to compress, while the leeward load causes the inner flange to compress.

In girt design, AISI S100 and AS/NZS 4600 provide guidelines to check for a combination of flexural strengths about two principal axes, with the nominal flexural strength about the major axis typically being dominant. The lateral bracing distance on the compressive flange governs this strength. The outer flange is always fastened to the sheathing, which effectively prevents lateral displacement. For corrugated iron, the bracing distance equals the distance between screws. The inner flange, however, is typically free (unbraced, except in cases of double sheathing), meaning the bracing distance can equal the girt span, which is often much larger than that of the outer flange. When the inner flange is in compression, the nominal flexural strength is primarily governed by global buckling strength (lateral-torsional buckling for flexural members), which can decrease significantly, making the case more unfavorable. For symmetrical sections like channels, the imbalance in strengths in opposite directions can lead to material waste.

* Corresponding author: anhvq@hau.edu.vn

<http://dx.doi.org/10.28991/CEJ-2024-010-11-05>



© 2024 by the authors. Licensee C.E.J, Tehran, Iran. This article is an open access article distributed under the terms and conditions of the Creative Commons Attribution (CC-BY) license (<http://creativecommons.org/licenses/by/4.0/>).

There are solutions to improve the global buckling strength of cold-formed C-section girts when the inner flange is in compression. These solutions are generally categorized into two approaches: increasing cross-sectional dimensions and reducing lateral bracing length [1]. The most common bracing method for girts with the inner flange in compression is the application of tie rods (or sag rods). Some studies have examined the effectiveness of tie rods [2-5]. Birkemoe et al. [2] and Polyzois & Birkemoe [3] conducted full-scale tests of wall panels with girts, demonstrating the effectiveness of sag rods and panels as stiffening and strengthening agents for channel and Zee sections with unsupported compression flanges. These tests also showed that the midspan rotation of the girt, when the tie rod is placed near the compression flange, is significantly smaller than when placed at the mid-web. Polyzois & Birkemoe [4] further recommended a stress analysis technique for the design of girts and purlins, accounting for the contributions of wall or roof material, intermediate restraint, and end supports. The effective stiffness of tie rods was also studied, considering the local deformation of the web [6].

Another approach to reducing the lateral bracing length is to strengthen the support conditions. Overlapping profiles is a common solution for Zee cross-sections, and studies have been conducted to improve the connection. Andrei Gîrbacea & Ungureanu [7] performed experiments and finite element simulations on two-span purlins with sheathing to investigate overlap length. They found that an overlap length of 15% to 25% of the purlin span is the most effective. For channel cross-sections, sleeve connections are used instead of overlaps due to the complexity of overlapping. Bondapalli et al. [8] recently conducted 180 finite element simulations on sleeve connections between C-section flexural members, showing that a sleeve length of 3.5 times the cross-section depth can fully transfer the moment over the support.

Increasing the size of the girts improves buckling strength, whether the outer or inner flange is in compression. Notably, the AISI S100 [9] and AS/NZS 4600 [10] have a specific section introducing a reduction factor, or R -value, which accounts for the bracing effect of sheathing on the inner flange. This approach, based on experimental results from studies by Peköz & Soroushian [11] and Soroushian & Peköz [12], LaBoube [13], Haussler & Pabers [14], LaBoube et al. [15], Haussler [16], and Fisher [17], is also referenced in other design guidelines [1, 18, 19]. More experiments continue to refine this approach. For example, Wibbenmeyer Kaye Dee determined the R -values for Z-purlins and girts with through-fastened panels having dimensions falling outside the limits of the current specification [20]. Luan & Li [21] tested purlin roof assemblies under uplift wind loads. Tian Gao examined the rotational restraint provided to wall girts and roof purlins by through-fastened metal panels [22-24].

While various methods have been proposed to improve the global buckling strength of girts or purlins under bending about their asymmetrical axis when the inner flange is in compression, these methods are often scattered across different studies, limiting their practical application for designers. Furthermore, although there are studies on tie rods and sheathings, no comprehensive parametric study has been conducted on girts with the inner flange in compression. Therefore, this paper first summarized the solutions for improving the lateral buckling strength of girts with the inner flange in compression and then examined the influence of girt geometric parameters on global buckling strength.

The study confronted some difficulties and challenges:

- For methods to improve the global buckling strength of girts or purlins: These methods are scattered across different literature.
- For the influence of girt geometric parameters on global buckling strength: Many geometric parameters can influence this strength. A massive set of cross-sections needs to be investigated, which requires an automatic approach to solve the problem.

In this study, a semi-automatic method based on the closed-form formulae of AISI S100 design code with the aid of Microsoft Excel was used to deal with the second challenge. 63 problems generated from the three Lysaght pre-fabricated channel cross-sections when changing four major cross-sectional dimensions were solved to provide transparent results for discussion

2. Solutions to Improve the Flexural Strength of Girts with an Inner Flange in Compression

2.1. Increasing Cross-Section Dimensions

Cold-formed channel cross-sections are defined by several geometric parameters: section height (D), flange width (B), lip height (L_f), section thickness (t), and inner bending radius (R), as shown in Figure 1. Except for the inner bending radius (R), increasing any of these dimensions results in improved section properties, which can reduce the slenderness of the member, thereby enhancing flexural strength. The influence of these parameters on flexural strength will be examined in more detail in the next section.

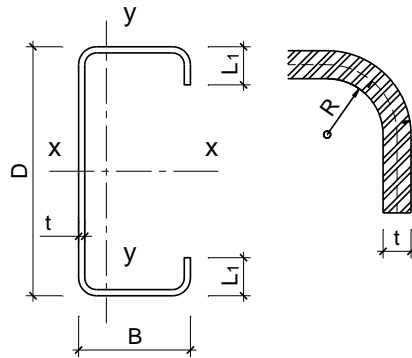


Figure 1. Cross-section parameters

2.2. Reducing Bracing Distances

Installing tie rods connecting the webs of channel girts, as shown in Figure 2-a, can reduce the bracing distances. Flat straps, as shown in Figure 2-b, are another option, borrowed from the lateral bracing of cold-formed columns [1]. This approach is more efficient than tie rods, as flat straps connect the wall girts through the inner compressive flanges.

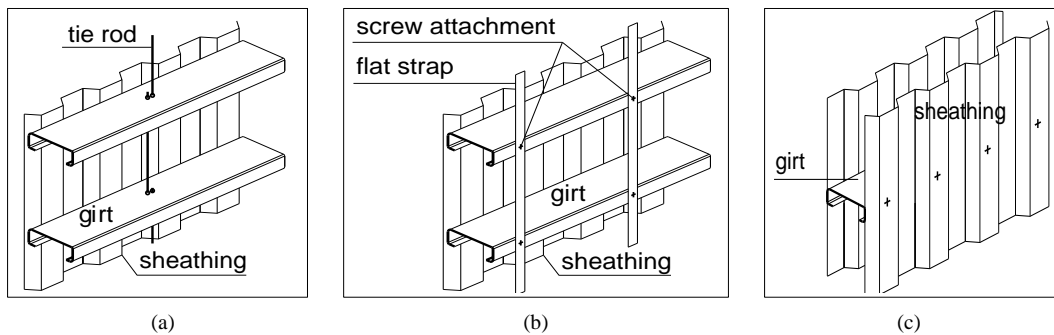


Figure 2. Installation of inner lateral braces

In some buildings, double sheathings are required for insulation, as shown in Figure 2-c. This naturally provides bracing to the inner flanges of girts.

A sub-column in Figure 3 reduces the girt span. It affects not only the bracing length of the inner flange under the leeward wind load but also the span of the girts under the windward wind load.



Figure 3. Reducing the span of girts by using sub-frames

2.3. Strengthening the End Connections

Wall girts are commonly simply supported for ease of installation. To reduce the effective length of girts, end connections can be modified to increase stiffness. An approach recommended by the authors is shown in Figure 4, where a connector (in this case, a flat plate) links the ends of two girts. It should be noted that to improve the global buckling strength of girts when the inner flange is in compression, only the inner flange needs to be connected, not the entire cross-section.

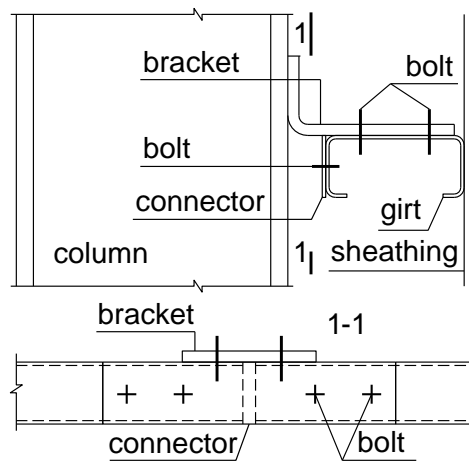


Figure 4. Strengthening the fixity of the two ends

Another strengthening approach applied to purlins, such as overlapping (or bypassing), using sleeve connectors, or installing fly bracing, can also be considered for girts.

2.4. Consideration of the Bracing Effect of Sheathing on the Inner Compressive Flange

For wall girts subjected to wind suction, where the outer flange is fastened to sheathing and the inner flange is free, the flexural strength lies between the strengths of fully braced and unbraced members. The restraint depends on the rotational stiffness of the connection between panels and girts. AISI S100 and AS/NZS 4600 provide factors that account for strength reduction compared to a fully braced state. These factors are detailed in Section I6.2.1 for girts and purlins with the outer flange attached to the wall panel. For purlins in standing seam roofs, these factors are listed in Sections I6.2.2.

The nominal strength, M_n , of a channel bent about the asymmetrical x -axis, when the flange connected to the sheathing is in tension and the remaining flange is compressive and free can be computed as follows (Equation 1)

$$M_n = RM_{nlo} \tag{1}$$

where R is the reduction factor obtained from Table 1.

Table 1. The reduction factor, R

Number of spans	Member depth range, d (mm)		
	$d \leq 165$	$165 < d \leq 216$	$216 < d \leq 305$
Simple	0.70	0.65	0.40
Continuous	0.60		

M_{nlo} - nominal flexural strength (i.e., M_{nl}) considering only the local buckling. It is outlined in Section F3 of AISI S100 where the distortional buckling is excluded and applying $F_n = F_y$ (also means $M_{ne} = M_y$). The limitation of using the reduction factor, R , is listed in Section I6.2.1. If the scope of the application is not satisfied, full-scale tests (see Section K2.1 of AISI S100) or a rational engineering analysis can be used to determine this value. It should be noted that cantilever beams and some parts of a continuous beam are not allowed to utilize this effect (refer to AISI S100 for more details). Bracing and boundary conditions do not affect the value of M_n . Only variations in cross-sectional dimensions can change the value of the reduction factor R and the local buckling moment M_{nlo} , ultimately causing M_n to increase or decrease.

The following sections will discuss the influence of cross-sectional dimensions on the lateral-torsional buckling strength when the unbraced inner flange is in compression.

3. Sampling plan for Assessing Geometric Parameters on the Lateral-Torsional Buckling Strength

Three typical thin-walled, cold-formed girts with cross-sections ($D \times B \times L_1 \times t$) of C102×51×14.5×1.2, C203×76×21×2.4, and C300×96×31.5×3 (arranged by increasing size) were taken from Lysaght’s catalog [25] with an inner fillet radius $R = 5$ mm. The girts were modeled as simply supported beams in both principal directions, with span length $L = 6$ m and spacing $s = 1.2$ m. The girts were fastened to steel panels with a fastener spacing of $s_f = 0.3$ m, and a vertical brace was installed at the midspan, resulting in an inner flange bracing length of 3 m. The material properties of the girts were assumed to include an elastic modulus $E = 200000$ MPa, Poisson ratio $\nu = 0.3$, and yield strength $F_y = 450$ MPa. The design negative (leeward) wind pressure was -2.295 kN/m² (equivalent to a basic wind speed of 56.7 m/s on flat terrain, exposure category “D”). The setup is illustrated in Figure 5.

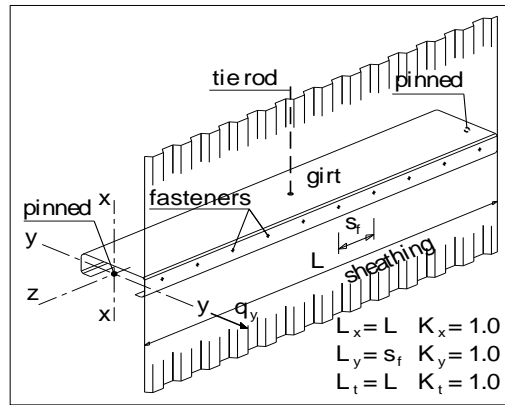


Figure 5. Girt settings

The Direct Strength Method (DSM) as outlined in AISI S100-16 [9] was used to design the girts.

Based on these typical cross-sections, geometric parameters were varied to match the built-in cross-sections of Lysaght [25], as shown in Table 2.

Table 2. Range of values (mm)

Parameters	Values								
<i>D</i>	102	152	203	254	300				
<i>B</i>	51	64	76	96	125				
<i>L₁</i>	12.5	14.5	16.5	18.5	21	27.5	30	31.5	
<i>t</i>	1	1.2	1.5	1.9	2.4	3			

For wall girts with an unbraced inner flange in compression, two available flexural strengths (factored resistances) must be calculated: one considering the sheathing effect and one without sheathing effects based on Sections I6.2 (or Equation 1) and F1 of AISI S100, respectively. The resistance factors are consistent across all cases, so nominal strengths can be used for comparison instead of ultimate strengths. For the nominal strength without considering sheathing effects, it was observed that the nominal flexural strength accounting for the interaction between local buckling and global buckling M_{nl} governs all three investigated cross-sections. Thus, a direct comparison between M_n (Equation 1) and M_{nl} (Section F3.2.1) can provide further insights into the influence of sheathing.

The calculation flow for final nominal bending strength M_{nl_final} for girts bent about the x-axis, with the inner flange in compression, is shown in Figure 6 in reverse order. It represents the maximum of nominal strengths M_{nl} (without considering the sheathing effect) and M_n (considering the sheathing). M_{nl} is derived from the interaction between the yielding/global buckling moment M_{ne} and the local critical buckling moment M_{crl} , which is the minimum of moments causing local buckles of the web, flange, and lip, respectively. M_n is computed from M_{nol} , which represents the interaction between yielding moment M_y and M_{crl} .

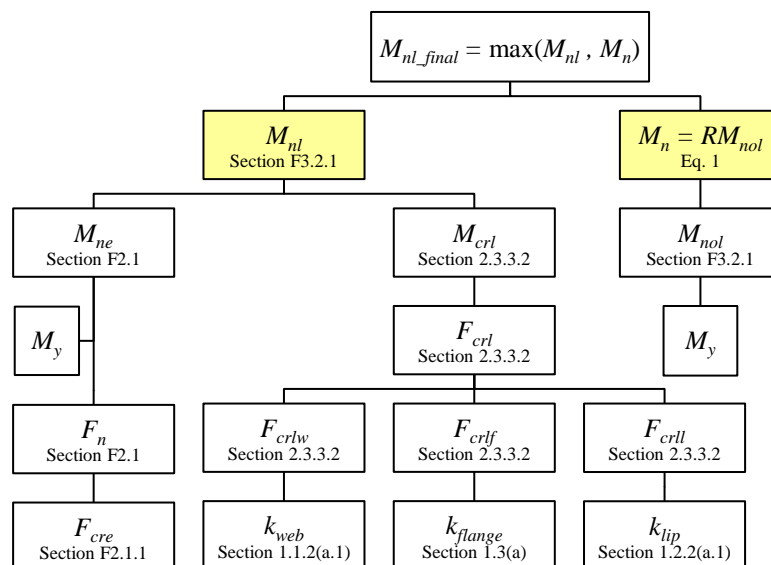


Figure 6. Calculation flow for nominal strength of major axis (x-x) bending

The section indices in the diagram refer to those outlined in the AISI S100 Specification. Other symbols, such as the global buckling stress F_{cre} and its global flexural stress F_n ; the local buckling stress F_{crit} (the minimum of the local buckling stress of the web F_{critw} , the flange F_{critf} , and the lip F_{critl} , which are determined from the corresponding buckling coefficients k_{web} , k_{flange} , and k_{lip} , respectively), are explained in the respective sections of the Specification.

The example above, using different parameters from Table 2, generated 63 problems, all of which were solved manually using Microsoft Excel.

4. Results and Discussions

4.1. Parameter Study

The nominal flexural strengths M_{nl} and M_n (in kN.m) for the 63 problems above are shown in Figures 7 to 10, with respect to flange width B , lip length L_l , section depth D , and section thickness t , all in mm. Each point on the graphs represents a problem. For example, the second point in the series $300 \times B \times 31.5 \times 3$ in Figure 7-a has the value of $B = 64$ mm and $M_{nl} = 14.1$ kN.m. This point is the result of the nominal flexural strength without considering the sheathing effect M_{nl} from the problem of cross-section $300 \times 64 \times 31.5 \times 3$.

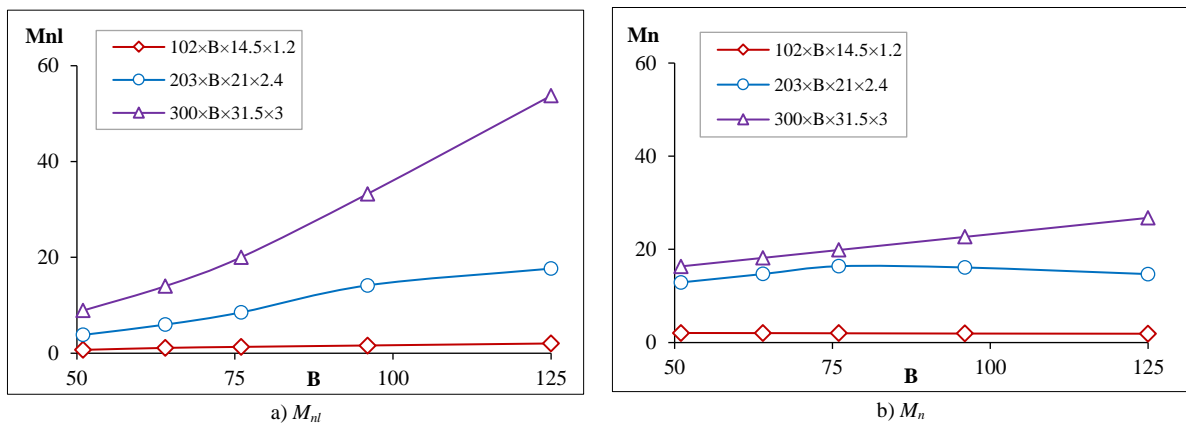


Figure 7. Variation of M_{nl} and M_n with respect to B

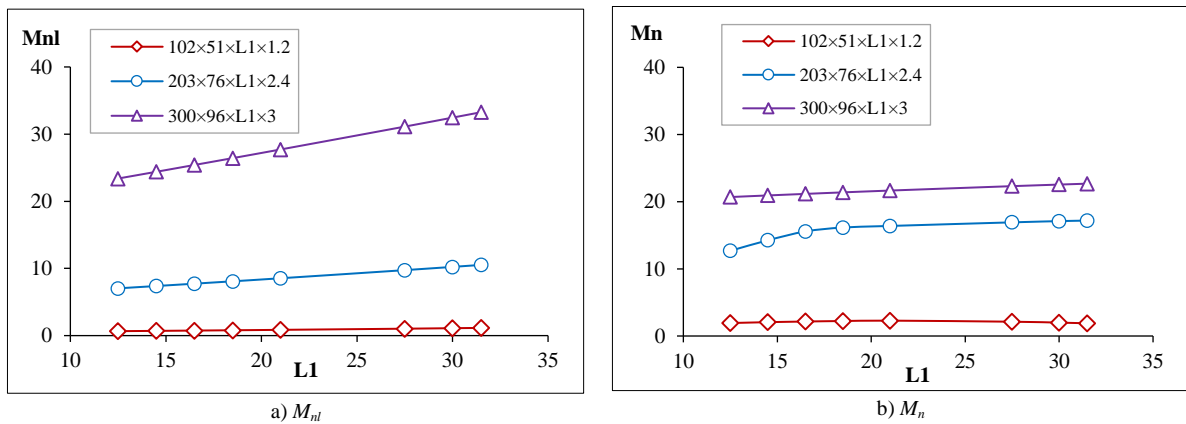


Figure 8. Variation of M_{nl} and M_n with respect to L_l

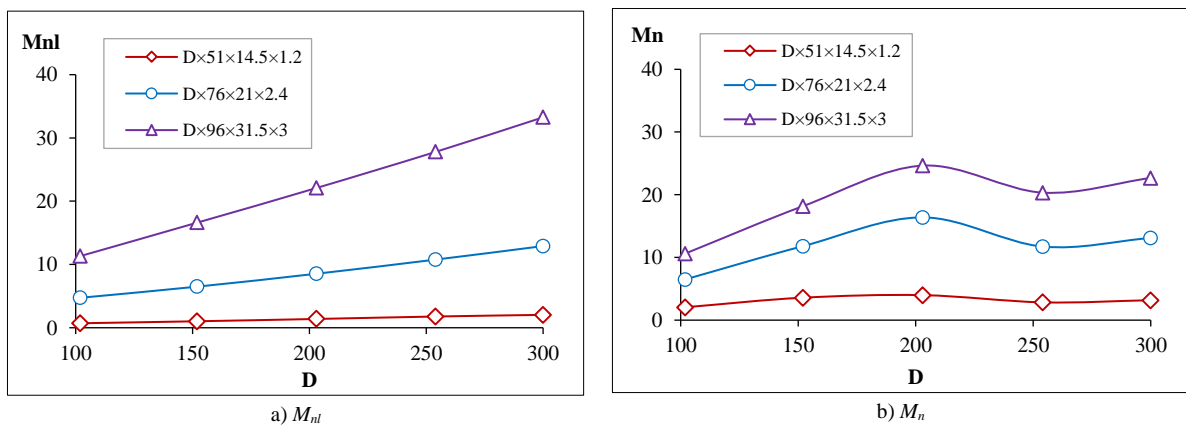


Figure 9. Variation of M_{nl} and M_n with respect to D

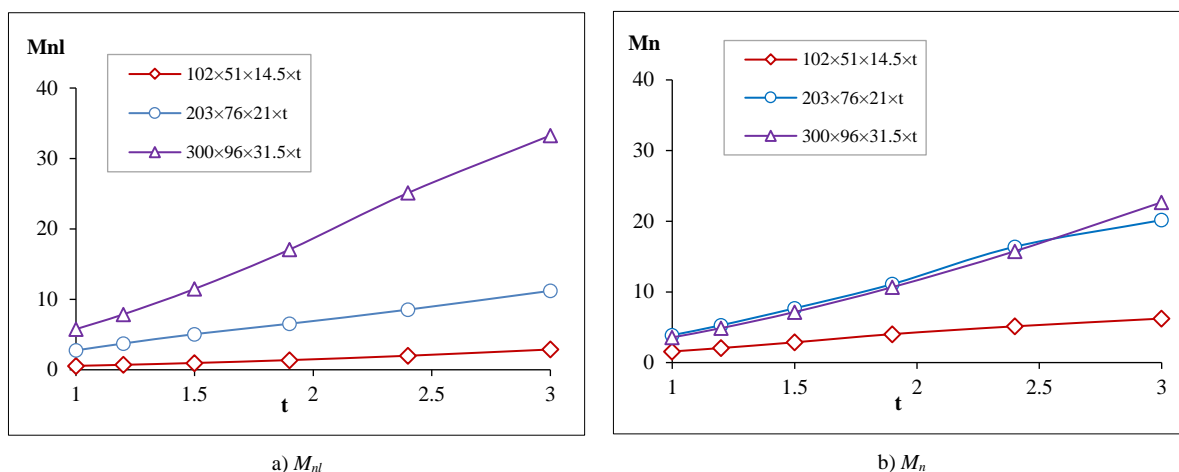


Figure 10. Variation of M_{nl} and M_n with respect to t

Since M_{nl} and M_n are unrelated, they are presented in separate diagrams and investigated independently. The final strength M_{nl_final} is simply a maximum of the two values and will be discussed in Section 4.3

It can be observed that the M_{nl} shows consistently increasing trends in all cross-sectional dimensions, even cross-sectional height D . The reason is that in the DSM method, M_{nl} is related to the section modulus S_f through the global buckling moment M_{ne} , which increases when the cross-sectional dimensions increase. All trend lines are virtually linear, so an almost constant slope can be obtained. For all dimensions, the magnitude and rate of change of M_{nl} always increase as the typical cross-sectional size increases. The rate of change for B is the highest, meaning that increasing B is the best way to improve M_n . The rate of change for L_1 is the lowest, and for t and D are almost the same, in which increasing t is slightly better, as shown in Table 3. It must be noted that to ensure the values are in the same context for comparison, parameter ratios, i.e., the ratio of a parameter to that of the first point, were used in the denominator of the rate of change equation instead of the parameters themselves.

Table 3. The rates of change of M_{nl} (kN.m per parameter ratio) with respect to section parameters

Section ID	B	L_1	D	t
102x51x14.5x1.2	0.9	0.3	0.7	1.2
203x76x21x2.4	9.5	2.3	4.2	4.2
300x96x31.5x3	30.9	6.5	11.3	13.7

The variations of M_n regarding cross-sectional dimensions are inconsistent, except for cross-section thickness. As B or L_1 increases, the section modulus increases, and the yield moment follows, however, the local buckling strength decreases, resulting in both an increasing and decreasing trend in the nominal strength M_n . The thicker the section, the greater the local buckling moment, the less it affects M_n , and the more stable the increasing trend of M_n (as shown by the top lines in Figures 7-b and 8-b), and vice versa.

The decreasing stage in the curves in the relationship between M_n and D (Figure 9-b) can be explained by the abrupt change of the reduction factor R in Table 1 from 0.65 to 0.4 when D is greater than 216 mm. Because the Specification does not provide a smooth change in R , the increasing trend of M_n in some parts of the curves in Figure 9-b is unreliable. M_n generally shows only an insignificant change as B , L_1 , or D varies. The increasing trend of M_n relating to t in Figure 10-b is the most steady and thus most reliable.

4.2. Efficiency Study

To assess the efficiency of varying cross-sectional dimensions, a weight ratio r_w was introduced. The weight of each problem was calculated, and the ratio of this weight to the weight of the corresponding typical section r_w was determined. This left r_w as the sole variable instead of the individual geometric parameters B , t , D , and L_1 , enabling the results to be displayed in a unified diagram. For clarity, the results were divided into two groups, one for M_{nl} (Figure 11-a) and one for M_n (Figure 11-b). Each group contains three diagrams corresponding to the three typical sections, with four series associated with B , t , D , and L_1 .

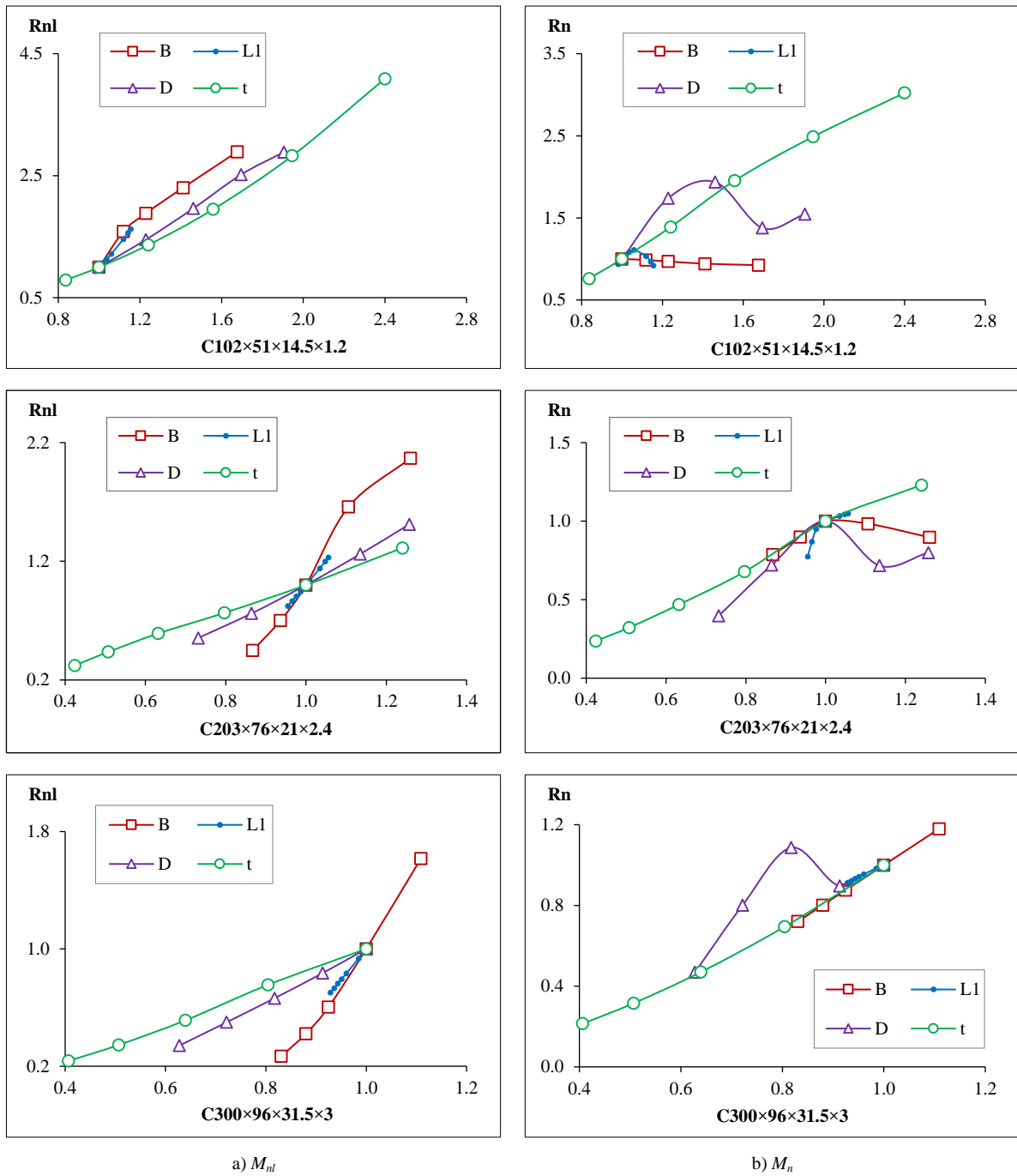


Figure 11. The change of M_{nl} and M_n with respect to the weight changing rate r_w

In these diagrams, curves with steeper slopes indicate better efficiency, as they reflect greater increases in flexural strength with minimal additional material consumption. And there is always a common point between the four series. This point (having $r_w = 1$) corresponds to the problem of a typical cross-section.

It can be seen from Figure 11-a that for M_{nl} , the slopes of curves of all typical cross-sections appear in the increasing order of t , D , L_1 , and B . As the cross-section size increases, the slope associated with a parameter increases, and the difference in slopes becomes more apparent. In contrast to the parameter study where changing t is a priority, the cross-section thickness gives the worst changing rate when considering material optimization. The reason is that the weight of the member increases rapidly along with the increase in M_n when changing t . The slopes of curves related to B and L_1 for all typical cross-sections are similar and the steepest, meaning that for increasing M_{nl} , increasing them consumes the smallest additional material. The curves related to B are slightly better and more reliable because the curves regarding L_1 are too short due to the narrow value range of the lip length investigated. In fact, only the inner flange width needs to be widened. Consequently, an asymmetric cross-section with a larger inner flange can be considered for wall girts to reduce the difference between the nominal strengths when the two flanges have significantly different bracing lengths, as shown in Figure 12. The above discussion is well illustrated by Figure 13.

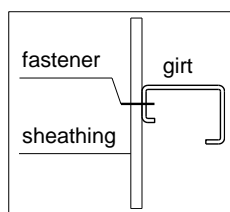


Figure 12. Asymmetric cross-section girt

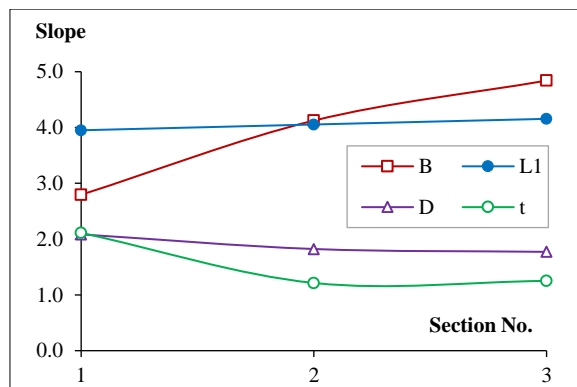


Figure 13. Slopes of curves in Figure 11-a (C102×51×14.5×1.2, 2 - C203×76×21×2.4, 3 - C300×96×31.5×3)

The relations of M_n with respect to B , D , and L_1 in Figure 11b are unstable and unreliable. In the first two cross-section diagrams, curves related to B and L_1 show an entirely or partly downward unfavorable trend. Only in the last cross-section diagram, positive slopes are prevalent and similar among parameters (with the slope of the series regarding D being conservatively obtained from two endpoints). This means that it is difficult to predict the behavior of M_n when changing D , B , or L_1 for smaller cross-sections. The situation is much better for larger cross-sections.

Among parameters, the curves corresponding to cross-section thickness t show a consistent increasing trend. Thus, increasing the section thickness is the best solution to improve the nominal strength of M_n . Interestingly, the slope of curves corresponding to t does not change too much, in the case of M_n as well as M_{nl} . These rates of change are about 1.2, as shown in Table 4.

Table 4. The rates of change of t series

No.	Section ID	For M_{nl}	For M_n
1	C102×51×14.5×1.2	2.11	1.45
2	C203×76×21×2.4	1.21	1.22
3	C300×96×31.5×3	1.25	1.28

4.3. Final Nominal Strength Discussion

It is emphasized that the final nominal bending strength M_{nl_final} is the maximum of M_{nl} and M_n . This means that the higher strength is utilized in the design, allowing for better strength mobilization. Using the lower value is more conservative but acceptable. By comparing the left-hand diagrams in Figures 7 to 10 to the right-hand diagrams, it can be seen that M_{nl} governs the final nominal flexural strength for the largest cross-section (C300×96×31.5×3), whereas M_n dominates in the smaller cross-sections (C102×51×14.5×1.2 and C203×76×21×2.4). This observation suggests that more extensive investigations into additional cross-sections could further confirm this trend.

5. Conclusions

Since the unbraced length of the inner flange of wall girts is typically much longer than that of the outer flange, the global buckling strength of the inner flange is significantly smaller. To address this, several solutions were discussed in this paper to improve the global buckling strength, including:

- Increasing the cross-sectional dimensions;
- Reducing the bracing distances;
- Strengthening the end connections;
- Considering the bracing effect of sheathing.

This paper also investigated the influence of cross-sectional dimensions on the nominal lateral buckling strengths (M_n and M_{nl}), both with and without considering the sheathing effect. This is particularly important, as lateral bracing and end fixities have little effect on M_n . The results revealed that M_{nl} governs the final nominal flexural strength of girts with the inner flange in compression for smaller cross-sections, whereas M_n is dominant in larger cross-sections. To improve M_{nl} , increasing the flange width was found to be the most effective method. Conversely, increasing the cross-section thickness is the best way to improve M_n , and this solution also enhances M_{nl} . Since M_{nl} and M_n are independent, designers must select an approach based on which nominal strength governs the design.

As a result, an asymmetric cross-section with a wider inner flange is appropriate for wall girts where the outer flange is fastened to sheathing and the inner flange is unbraced or less braced. The new cross-section requires further study in terms of design, fabrication, shipping, and installation to ensure it can be used effectively in practice.

6. Declarations

6.1. Author Contributions

Conceptualization, H.H.V., Q.A.V., and C.H.P.; methodology, H.H.V.; software, H.H.V.; validation, Q.A.V.; formal analysis, H.H.V.; investigation, C.H.P.; resources, Q.A.V.; data curation, C.H.P.; writing—original draft preparation, H.H.V.; writing—review and editing, Q.A.V. and C.H.P.; visualization, C.H.P.; supervision, H.H.V.; project administration, C.H.P. All authors have read and agreed to the published version of the manuscript.

6.2. Data Availability Statement

The data presented in this study are available in the article.

6.3. Funding

The authors received no financial support for the research, authorship, and/or publication of this article.

6.4. Conflicts of Interest

The authors declare no conflict of interest.

7. References

- [1] Sputo, T., & Turner, J. L. (2005). *Bracing Cold-Formed Steel Structures*. American Society of Civil Engineers (ASCE), Reston, United States. doi:10.1061/9780784408179.
- [2] Birkemoe, P. C., & Birkemoe, P. (1976). Behaviour and Design of Girts and Purlins for Negative Pressure. Proceedings Canadian Structural Engineering Conference, 18-23 July 1976.
- [3] Polyzois, D., & Birkemoe, P. C. (1985). Z- Section Girts Under Negative Loading. *Journal of Structural Engineering*, 111(3), 528–544. doi:10.1061/(asce)0733-9445(1985)111:3(528).
- [4] Polyzois, D., & Birkemoe, P. C. (1980). Behavior and Design of Continuous Girts and Purlins. Fifth International Specialty Conference on Cold-Formed Steel Structures, 18-19 November, St. Louis, United States.
- [5] Polyzois, D. (1987). Sag Rods as Lateral Supports for Girts and Purlins. *Journal of Structural Engineering*, 113(7), 1521–1531. doi:10.1061/(asce)0733-9445(1987)113:7(1521).
- [6] Zhang, L., & Tong, G. S. (2015). Stress analysis on cold-formed C-purlins subjected to wind suction load considering the effective stiffness of anti-sag bar. *Thin-Walled Structures*, 90, 107–118. doi:10.1016/j.tws.2014.12.022.
- [7] Andrei Gîrbacea, I., & Ungureanu, V. (2023). Efficient design of overlapped purlins loaded by gravity. *Structures*, 58. doi:10.1016/j.istruc.2023.105512.
- [8] Bondapalli, S. C., Natesan, V., & Madhavan, M. (2024). Numerical investigation of cold formed steel sleeve connection for channel sections subjected to combined bending and shear. *Journal of Constructional Steel Research*, 217. doi:10.1016/j.jcsr.2024.108588.
- [9] AISI S100. (2016). *North American Specification for the Design of Cold-Formed Steel Structural Members*. American Iron and Steel Institute (ASI), Washington, United States.
- [10] AS/NZS 4600:2005. (2005). *Cold-Formed Steel Structures*. Standards Australia/Standards New Zealand, Sydney, Australia.
- [11] Peköz, T., & Soroushian, P. (1981). Behavior of C- and Z-Purlins under Uplift. Report No. 81-2, Cornell University, Ithaca, United States.
- [12] Soroushian, P., & Peköz, T. (1982). Behavior of C-and Z-purlins under wind uplift. Proceedings of the Sixth International Specialty Conference on Cold-Formed Steel Structures, 16 November, 1982.

- [13] LaBoube, R. A. (1986). Roof panel to purlin connection: rotational restraint factor. International Association for Bridge and Structural Engineering (IABSE) Colloquium, June, 1986, Stockholm, Sweden.
- [14] Haussler, R. W., & Pabers, R. F. (1973). Connection strength in thin metal roof structures. 2nd International Specialty Conference on Cold-Formed Steel Structures, 22-24 October, 1973, St. Louis, United States.
- [15] LaBoube, R. A., Golovin, M., Montague, D. J., Perry, D. C., & Wilson, L. L. (1988). Behavior of continuous span purlin systems. 9th International Specialty Conference on Cold-Formed Steel Structures, 8-9 November, 1988, St. Louis, United States.
- [16] Haussler, R. W. (1988). Theory of cold-formed steel purlin/girt flexure. 9th International Specialty Conference on Cold-Formed Steel Structures, 8-9 November, 1988, St. Louis, United States.
- [17] Fisher, J. M. (1996). Uplift Capacity of Simple Span Cee and Zee Members with Through-Fastened Roof Panels. Final Report, MBMA 95-01, Metal Building Manufacturers Association, Ohio, United States.
- [18] AISI. (1997). A Guide for Designing with Standing Seam Roof Panels, Design Guide CF97-1. Committee on Specifications for the Design of Cold-Formed Steel Structural Members, American Iron and Steel Institute (AISI), Washington, United States.
- [19] Design Guide D111-09. (2011). Design Guide for Cold-Formed Steel Purlin Roof Framing Systems. Committee on Specifications for the Design of Cold-Formed Steel Structural Members, American Iron and Steel Institute (AISI), Washington, United States.
- [20] Wibbenmeyer, K. D. (2010). Determining the R values for 12 inch deep Z-purlins and girts with through-fastened panels under suction loading. Master Thesis, Missouri University of Science and Technology, Rolla, United States.
- [21] Luan, W., & Li, Y. Q. (2019). Experimental investigation on wind uplift capacity of single span Z-purlins supporting standing seam roof systems. *Thin-Walled Structures*, 144. doi:10.1016/j.tws.2019.106324.
- [22] Gao, T., & Moen, C. D. (2012). Predicting rotational restraint provided to wall girts and roof purlins by through-fastened metal panels. *Thin-Walled Structures*, 61, 145–153. doi:10.1016/j.tws.2012.06.005.
- [23] Gao, T., & Moen, C. D. (2012). Direct Strength Design of Metal Building Wall and Roof Systems-Through-fastened Simple Span Girts and Purlins with Laterally Unbraced Compression Flanges. 21st International Specialty Conference on Cold-Formed Steel Structures, 24-25 October, 2012, St. Louis, United States.
- [24] Gao, T., & Moen, C. D. (2014). Extending the Direct Strength Method for Cold-Formed Steel Design to Through-Fastened Simple Span Girts and Purlins with Laterally Unbraced Compression Flanges. *Journal of Structural Engineering*, 140(6). doi:10.1061/(asce)st.1943-541x.0000860.
- [25] Lysaght. (2014). Zeds and Cees User's guide for design and installation professionals. Lysaght, Sydney, Australia. Available online: <https://agnew-cdn.n2erp.co.nz/cdn/images/productdocument/LYT0063---2024-01-11---L1---User-Guide---Z.pdf> (accessed on October 2024).